Journal of Applied Fluid Mechanics, Vol. 11, No. 1, pp. 65-77, 2018.
Available online at www.jafmonline.net, ISSN 1735-3572, EISSN 1735-3645.
DOI: 10.29252/jafm.11.01.27519

Linear and Weak Nonlinear Double Diffusive Convection in a Viscoelastic Fluid Saturated Anisotropic Porous Medium with Internal Heat Source

A. Srivastava† and A. K. Singh

Department of Mathematics, Institute of Science, Banaras Hindu University, Varanasi-221005, India

†*Corresponding Author Email: srivastavaalok0311@gmail.com*

(Received December 19, 2017; accepted September 6, 2017)

ABSTRACT

This paper deals linear and weak nonlinear stability analysis of double-diffusive convection in an anisotropic porous layer with internal heat source saturated by viscoelastic fluid. For linear stability analysis we use normal mode technique and obtained the expression for oscillatory thermal Rayleigh number which is used to plot neutral stability curve for oscillatory case. For nonlinear analysis truncated representation of Fourier series upto two terms is used. The system of time dependent nonlinear equation is solved numerically and plot the curve for heat transfer and mass transfer with respect to time for different parameters. Effect of thermal anisotropy parameter, mechanical anisotropy parameter, relaxation parameter, retardation parameter, internal heat source parameter, solute Rayleigh number, diffusivity ratio, Darcy-Prandtl number on the onset of convection, heat and mass transfers have been discussed. We also draw the stream lines, isotherms, isohalines at different times.

Keywords: Internal heat source, Double-diffusive convection, Porous media, Anisotropic, Viscoelastic.

NOMENCLATURE

a	Wave number
d	depth of the fluid layer
Da	Darcy number
G	acceleration due to gravity
K_x	permeability in x-direction
K_z	permeability in z-direction
Nu	Nusselt number
P	reduced pressure
Pr	Prandtl number
Pr_D	Darcy-Prandtl number
Q	internal heat source
Ra_T.	Thermal Rayleigh number
Ra_S	Solute Rayleigh number
R_i	internal heat source parameter
S	solute concentration
ΔS	solute difference across the porous layer
Sh	Sherwood number
T	temperature
ΔT	temperature difference across the porous layer
t	time
x, y, z	space Co-ordinates
β_S	coefficient of solute expansion
β_T	coefficient of thermal expansion
λ_1	relaxation time
λ_2	retardation time
η	thermal anisotropy parameter
ξ	mechanical anisotropy parameter
κ_S	solutal diffusivity
κ_T	$\kappa_{Tx}(ii + jj) + \kappa_{Tz}(kk)$
κ_{Tx}	effective thermal diffusivity in x-direction
κ_{Tz}	effective thermal diffusivity in z-direction
τ	diffusivity ratio
μ	dynamic viscosity of the fluid
ϕ	porosity
ν	kinematic viscosity
ρ	fluid density
ψ	stream function

Other symbols

∇_1^2	$\frac{\partial^2}{\partial x^2}+\frac{\partial^2}{\partial y^2}$
∇^2	$\nabla_1^2+\frac{\partial^2}{\partial z^2}$

Subscripts

b	basic state
c	critical
0	reference value

superscripts

$'$	perturbed quantity

$*$	dimensionless quantity	*Osc*	oscillatory
F	finite amplitude	*St*	stationary

1. INTRODUCTION

Enough research papers are available on convection in porous media due to its wide range of application in filtration, bio-remediation, petroleum engineering, electrochemistry, geo-physical systems, Earth's mantle convection. Review in this area is collected and presented in a progressive way by Nield and Bejan (2013), Ingham and Pop (2005), Vadász (2008), Vafai (2005). Due to growing research in porous media, double-diffusive convection in porous media attracts many researchers in recent years because of its applications in atmospheric science, seawater flow, earth's mantle convection, solidification of binary alloys. The work of Nield (1968) provide a base in this area and was continued by Griffiths (1981), Rudraiah *et al.* (1982), Poulikakos (1986), Murray and Chen (1989), Mulone and Straughan (2006).

Study related to Newtonian fluid are large however viscoelastic fluid attracts less attention of researchers. Now in days viscoelastic fluids are highly used in modern industries, carbon dioxide geologic sequestration. Stability of viscoelastic fluid in densely packed porous layer saturated has been investigated by Rudraiah *et al.* (1989), Wang and Tan (2008) analysed linear stability of Maxwell fluid, Zhang *et al.* (2008) studied linear and nonlinear stability analysis of Oldroyd-B fluid in horizontal porous layer, Shivakumara and Sureshkumar (2007) studied the stability analysis of Oldroyd-B binary fluid with quadratic drag and throughflow, Narayana *et al.* (2012) investigated the linear and nonlinear stability analysis of binary Maxwell fluid including cross diffusion effect, Malashetty *et al.* (2009) analyses stability of binary viscoelastic fluid in an anisotropic porous layer, Malashetty and Kulkarni (2009) studied the thermal instability for viscoelastic fluid by taking Darcy-Brinkman-Maxwell and thermal non-equilibrium model and found that the first convective instability is oscillatory instead of stationary, Sekhar and Jayalatha (2010) analysed elastic effect on Rayleigh-Bénard convection with temperature dependent viscosity, Kang *et al.* (2011) has been studied the effect of rotation for the viscoelastic fluid by considering the Darcy-Maxwell-Jeffrey model and they found that the effect of rotation is to reduce the heat transfer capacity for stationary as well as for overstable convection modes, Narayana *et al.* (2013) studied the effect of magneto convection on the viscoelastic fluid of type Oldroyd-B by using Lorenz system.

Most of the study in relevant area are mainly dealt with isotropic porous media, however there are many physical situations where thermal and mechanical anisotropy exists in porous matrix, one of such example is our geothermal environment. Anisotropy is generally a consequence of preferential orientation of asymmetric geometry of porous matrix or fibres and is in fact encountered in numerous systems in industry and nature, also in artificial porous matrix anisotropy can be made deliberately according to applications. There are large number of practical situations in which convection is driven by internal heat source. The internal heating of the earth creates a temperature gradient between the interior and the exterior of the earth's crust which causes convection in the earth crust also application of internal heat source may be found in radioactive decay of unstable isotopes, metal waste form development for spent nuclear fuel, weak exothermic reaction which can take place within porous materials moreover internal heat source is the main energy source of celestial bodies which is generated by radioactive decay and nuclear reaction. Earlier work related to internal heat source in porous media are given by Tveitereid (1977) obtained the steady solution in the form of hexagons and two dimensional rolls for convection in a horizontal porous layer with internal heat source, Bejan (1978) studied analytically the buoyancy induced convection with internal heat source. Later Parthiban and Patil (1995) found that the internal heat source advances the on-set of convection under the effect of non-uniform boundaries temperatures, Alex *et al.* (2001) studied the thermal instability in porous media by taking variable gravity with internal heat source and found that the stationary longitudinal mode is favourable mode for the onset of convection, Hill (2005) studied the linear and nonlinear effect of concentration based internal heat source on the stability for double diffusive convection by using Darcy model, Saravanan (2009), Cookey *et al.* (2010) found that the internal heat source parameter destabilizes the onset of stationary convection in a low Prandtl number, Nouri-Borujerdi *et al.* (2007) analyses the effect of uniform heat source for the thermal nonequilibrium model, Nouri-Borujerdi *et al.* (2008) studied the instability with uniform heat generation and including the Brinkman term, Capone *et al.* (2011) studied the penetrative convection in the presence of internal heat source in an anisotropic porous layer with a constant through flow via internal heat source. Bhadauria *et al.* (2011) studied the effect of internal heat source in rotating anisotropic porous layer, Bhadauria (2012) investigated the effect of internal heat source on double diffusive convection in anisotropic porous layer, Bhadauria *et al.* (2013) analyses the effect of internal heat source in their nonlinear gravity modulation analysis and re-ported that internal heat source increases heat trans-port, Gaikwad and Kouser (2013) studied the effect of internal heating on the onset of convection for binary viscoelastic Oldroyd-B fluid using Darcy Brinkman model for isotropic porous media, Altawallbeh *et al.* (2014) has been studied the linear and nonlinear effect of internal heat source by taking anisotropic porous media and Soret effect, Srivastava *et al.* (2014) studied the linear and nonlinear effect of internal heat source for couple stress fluid saturated anisotropic porous layer, Gaikwad and Kouser (2014) analyses the internal heat source effect on the couple stress fluid, Bhadauria (2016) analyses the chaotic convection for viscoelastic fluid in the presence of heat source. To the best of

authors knowledge there is no available article which deals the linear and nonlinear stability analysis for the double diffusive convection in an anisotropic porous media saturated with viscoelastic fluid of type Oldroyd-B.

Viscoelastic fluids finds its application in modern industries, paint and auto-mobile industries, enhanced oil recovery, geothermal reservoirs, also some biological fluid falls in this category. Internal heat of the earth causes convection in earth's mantle, also in the solidification of metals there is a temperature difference between upper and lower layer which is caused by internal heat source. Double diffusive convection occurs very commonly in nature and many engineering problems and in the present context, is of interest in the study of extraction of metals from ores where a mushy layer is formed during solidification of a metallic alloy, to understand the geothermal processes, and in some biological applications where convection is driven by internal heat source. Further, most of the earlier studies kept porous medium as a isotropic porous medium, however in nature, the permeability of the porous medium is anisotropic. Therefore, in this paper we consider the effect of internal heat source for double diffusive convection in an infinitely extended horizontal anisotropic porous layer saturated with viscoelastic fluid.

2. GOVERNING EQUATIONS

We consider an infinite horizontal anisotropic porous layer saturated by viscoelastic fluid confined between the planes z = 0 and z = d with internal heat source, which is heated and salted from be-low. We choose Cartesian frame of reference as, origin in the lower boundary and the z-axis in vertically upward direction. The gravity force is acting in vertically downward direction, we consider only free-free boundaries. We consider laminar flow, under steady-state flow conditions, homogeneous fluid, isotherm and incompressible, fluid phase and solid phase are in local thermal equilibrium. It is assumed that the mechanical properties and thermal properties in x and y directions are same. Uniform adverse temperature gradient ΔT/d and concentration gradient ΔS/d are maintained across the surfaces. Further the density variation is considered under Boussinesq approximation. The governing equations under the above considerations are given by

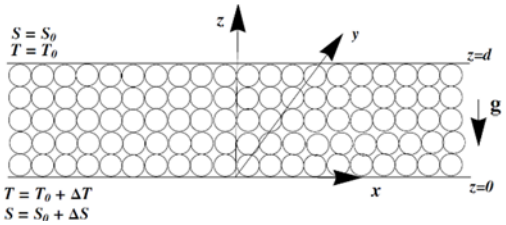

Schematic of the flow configuration.

$$\nabla . q = 0, \tag{1}$$

$$\left(1+\overline{\lambda_1}\frac{\partial}{\partial t}\right)\left(\frac{\rho_0}{\phi}\frac{\partial q}{\partial t}+\nabla p-\rho g\right)=-\mu\left(1+\overline{\lambda_2}\frac{\partial}{\partial t}\right)Kq, \tag{2}$$

$$\gamma\frac{\partial T}{\partial t}+(q.\nabla)T=\nabla.(\kappa_T\nabla T)+Q(T-T_0) \tag{3}$$

$$\phi\frac{\partial S}{\partial t}+(q.\nabla)S=\kappa_S\nabla^2 S, \tag{4}$$

$$\rho=\rho_0\left[1-\beta_T(T-T_0)+\beta_S(S-S_0)\right] \tag{5}$$

The thermal and solutal boundary conditions are

$$T=T_0+\Delta T \quad at\ z=0\ and\ T=T_0\ at\ z=d, \tag{6}$$

$$S=S_0+\Delta S\ at\ z=0 and\ S=S_0 at\ z=d. \tag{7}$$

The basic state of liquid is quiescent and given by

$$\begin{aligned} &q_b=0, p=p_b(z), T=T_b(z),\\ &S=S_b(z), \rho=\rho_b(z), \end{aligned} \tag{8}$$

which satisfy the following equations

$$\kappa_T\frac{d^2(T_b-T_0)}{dz^2}+Q(T_b-T_0)=0, \tag{9}$$

$$\frac{d^2S_b}{dz^2}=0, \tag{10}$$

$$\frac{\partial p_b}{\partial z}=-\rho_b g, \tag{11}$$

$$\rho_b=\rho_0\left[1-\beta_T(T-T_0)+\beta_S(S-S_0)\right]. \tag{12}$$

The solution of the Eq. (9), subject to the boundary conditions (6), is given by

$$T_b=T_0+\Delta T\frac{\sin\sqrt{Qd^2/\kappa_{Tz}}\left(1-\frac{z}{d}\right)}{\sin\sqrt{Qd^2/\kappa_{Tz}}} \tag{13}$$

Also by solving the Eq. (10) has been solved subjected to the boundary conditions (7), we get

$$S_b=S_0+\Delta S\left(1-\frac{z}{d}\right) \tag{14}$$

We use following transformations for non-dimensionalization:

$$\begin{aligned} &(x,y,z)=(x^*,y^*,z^*)d, t=t^*\left(\gamma d^2/\kappa_{Tz}\right),\\ &(u,v,w)=(u^*,v^*,w^*)\left(\frac{\kappa_{Tz}}{d}\right), T=(\Delta T)T^*,\\ &S=(\Delta S)S^*. \end{aligned} \tag{15}$$

Introducing the stream function in the form $(u,v,w)=\left(\frac{\partial\psi}{\partial z},0,-\frac{\partial\psi}{\partial x}\right)$ in Eqs. (2-4) then, taking curl to eliminate pressure term from Eq. (2) and then nondimensionlizing the resulting equations by using transformations given by Eq. (15). Finally we set γ = 1 and get the set of following equations

$$\left(1+\lambda_1\frac{\partial}{\partial t}\right)\left(\frac{1}{\mathrm{Pr}_D}\frac{\partial}{\partial t}\nabla^2\psi+Ra_T\frac{\partial T}{\partial x}-Ra_S\frac{\partial S}{\partial x}\right)+\left(1+\lambda_2\frac{\partial}{\partial t}\right)\left(\nabla_1^2+\frac{1}{\xi}\frac{\partial^2}{\partial z^2}\right)\psi=0, \tag{16}$$

$$\frac{\partial T}{\partial t}-\left(\eta\frac{\partial^2}{\partial z^2}+\frac{\partial^2}{\partial z^2}+R_i\right)T-\frac{\partial(\psi,T)}{\partial(x,z)}-\frac{\partial \mathrm{T}_b}{\partial z}\frac{\partial\psi}{\partial x}=0, \tag{17}$$

$$\frac{\partial S}{\partial t}-\tau\nabla^2 S-\frac{\partial(\psi,S)}{\partial(x,z)}+\frac{\partial\psi}{\partial x}=0. \tag{18}$$

where $\mathrm{Pr}_D=\frac{\phi\,\mathrm{Pr}}{Da}$ is Darcy-Prandtl number ($\mathrm{Pr}=\frac{\nu}{\kappa_{Tz}}$ is Prandtl number and $Da=\frac{K_z}{d^2}$ is Darcy number), $Ra_T=\frac{\beta_T g\Delta T d K_z}{\nu\kappa_{Tz}}$ is thermal Rayleigh number, $Ra_S=\frac{\beta_S g\Delta S d K z}{\nu\kappa_{Tz}}$ is solute Rayleigh number, $R_i=\frac{Qd^2}{\kappa_{Tz}}$ is internal heat source parameter, $\lambda_1=\frac{\kappa_{Tz}}{d^2}\overline{\lambda_1}$ is relaxation parameter, $\lambda_2=\frac{\kappa_{Tz}}{d^2}\overline{\lambda_2}$ is retardation parameter, $\tau=\frac{\kappa_S}{\kappa_{Tz}}$ is diffusivity ratio, $\xi=\frac{K_x}{K_z}$ is mechanical anisotropy parameter, $\eta=\frac{\kappa_{Tx}}{\kappa_{Tz}}$ is thermal anisotropy parameter.

The stress free, isothermal, isohalines boundary conditions are given by

$$\psi=\frac{\partial^2\psi}{\partial z^2}=T=S=0\ at\ z=0,1. \tag{19}$$

3. LINEAR STABILITY ANALYSIS

We linearise the Eqs. (16-18) by taking the Jacobian term equal to zero. To solve the eigenvalue problem defined by Eqs. (16-18), subject to the boundary conditions given by Eq. (19) by taking time periodic disturbance in horizontal plane, for the fundamental mode, we have

$$\begin{pmatrix}\psi\\T\\S\end{pmatrix}=e^{\sigma t}\begin{pmatrix}\psi_0\sin(ax)\\\Theta_0\cos(ax)\\\Phi_0\cos(ax)\end{pmatrix}\sin(\pi z), \tag{20}$$

where a is the horizontal wave number and $\sigma=\sigma_r+i\sigma_i$ is growth rate and in general a complex quantity. Substituting Eq. (20) in Eqs. (16-18) and setting the Jacobian term equal to zero, we obtained the non trivial solution in the form of the thermal Rayleigh number as follows:

$$Ra_T=\frac{\left(R_i-\left(\sigma+\delta_2^2\right)\right)}{2a^2F}\left[\frac{\delta^2\sigma}{\mathrm{Pr}_D}+\frac{(1+\lambda_2\sigma)\delta_1^2}{(1+\lambda_1\sigma)}+\frac{a^2Ra_S}{\left(\sigma+\tau\delta^2\right)}\right] \tag{21}$$

Where

$\delta^2=\pi^2+a^2$, $\delta_1^2=\frac{\pi^2}{\xi}+a^2$,

$\delta_2^2=\pi^2+\eta a^2$, $F=\int_0^1\frac{dT_b}{dz}\sin^2(\pi z)dz$.

For neutral stability state $\sigma_r=0$, whereas for $\sigma_r<0$ system is always stable and for $\sigma_r>0$ system is always unstable.

3.1 Stationary State

The expression of thermal Rayleigh number for the onset of stationary convection at the marginally stable steady state, for which the exchange of stabilities are valid correspond to the $\sigma=0$(i.e $\sigma_r=0$ and $\sigma_i=0$) becomes

$$Ra_T^{St}=\frac{\left(R_i-\delta_2^2\right)}{2a^2F}\left[\delta_1^2+\frac{a^2Ra_S}{\tau\delta^2}\right] \tag{22}$$

3.2 Oscillatory State

To obtain the expression of thermal Rayleigh number for oscillatory convection at the marginal state we have to substitute $\sigma=i\sigma_i$ (since the real part of σ for marginal oscillatory state is zero i.e $\sigma_r=0$) in Eq. (21) and clearing the complex quantity from denominator. After some simple simplification we have

$$Ra_T^{osc}=\Delta_1+i\,\sigma_i\Delta_2 \tag{23}$$

Where

$$\Delta_1=\frac{1}{2a^2F}\left[\frac{\delta^2\sigma^2}{\mathrm{Pr}_D}+\frac{\left(R_i-\delta_2^2\right)\left(1+\lambda_1\lambda_2\sigma^2\right)+\sigma^2\left(\lambda_2-\lambda_1\right)\delta_1^2}{\left(1+\lambda_1^2\sigma^2\right)}+\frac{a^2Ra_S\delta^2\tau\left(R_i-\delta_2^2\right)-\sigma^2}{\left(\delta^4\tau^2+\sigma^2\right)}\right], \tag{24}$$

and

$$\Delta_2=\frac{1}{2a^2F}\left[\frac{\delta^2\left(R_i-\delta_2^2\right)}{\mathrm{Pr}_D}+\frac{\left(R_i-\delta_2^2\right)\left(\lambda_2-\lambda_1\right)-\left(1+\lambda_1\lambda_2\sigma^2\right)\delta_1^2}{\left(1+\sigma^2\lambda_1^2\right)}-\frac{a^2Ra_S\left(R_i-\delta_2^2\right)+\delta^2\tau}{\left(\delta^4\tau^2+\sigma^2\right)}\right] \tag{25}$$

For oscillatory onset of convection, we have $\Delta_2 = 0$ (since Ra_T is a physical quantity therefore it must be real, also $\sigma \neq 0$ for oscillatory convection) this condition gives a biquadratic equation in σ

$$f\left(\sigma^2\right)^2 + g\left(\sigma^2\right) + h = 0 \tag{26}$$

Where

$$f = \lambda_1\left(\delta^2\left(R_i - \delta_2^2\right)\lambda_1 - \mathrm{Pr}_D\,\delta_1^2\lambda_2\right) \tag{27}$$

$$\begin{aligned} g = &-\mathrm{Pr}_D\,\delta_1^2 + \delta^2\left(R_i - \delta_2^2\right) + \delta^6\tau^2\left(R_i - \delta_2^2\right)\lambda_1^2 \\ &- a^2\,\mathrm{Pr}_D\,Ra_S\left(\delta^2\tau + R_i - \delta_2^2\right)\lambda_1^2 - \delta^4\tau^2\,\mathrm{Pr}_D\,\delta_1^2\lambda_1\lambda_2 \\ &+ \mathrm{Pr}_D\,\delta_1^2\left(R_i - \delta_2^2\right)\left(-\lambda_1 + \lambda_2\right), \end{aligned} \tag{28}$$

$$\begin{aligned} h = &-\delta^4\tau^2\,\mathrm{Pr}_D\,\delta_1^2 + \delta^6\tau^2\left(R_i - \delta_2^2\right) \\ &- a^2\,\mathrm{Pr}_D\,Ra_S\left(\delta^2\tau + \left(R_i - \delta_2^2\right)\right) \\ &+ \delta^4\tau^2\,\mathrm{Pr}_D\,\delta_1^2\left(R_i - \delta_2^2\right)\left(-\lambda_1 + \lambda_2\right); \end{aligned} \tag{29}$$

$$R_{a_T}^{Osc} = \frac{1}{2a^2F}\left[\frac{\delta^2\sigma^2}{\mathrm{Pr}_D} + \frac{\left\{\left(R_i - \delta_2^2\right)\left(1 + \lambda_1\lambda_2\sigma^2\right) + \sigma^2\left(\lambda_2 - \lambda_1\right)\right\}\delta_1^2}{\left(1 + \lambda_1^2\sigma^2\right)} + \frac{a^2Ra_S\left\{\delta^2\tau\left(R_i - \delta_2^2\right) - \sigma^2\right\}}{\left(\delta^4\tau^2 + \sigma^2\right)}\right], \tag{30}$$

4. WEAK NONLINEAR ANALYSIS

Though linear stability analysis is significant, but some important physical quantities like value of convection amplitude, heat transfer, mass transfer cannot be calculated using linear stability analysis, thus we need to do nonlinear stability analysis of the system. Nonlinear stability analysis provides useful information which help to describe the physical mechanism of convective flow with minimum amount of mathematics.

Nonlinear effect is to distort the temperature and concentration fields through the interaction of ψ and T, and ψ and S respectively, consequently a component of the form sin $(2\pi z)$ will be generated. We use minimal Fourier series representation to describe the finite amplitude in case of double-diffusive convection, as

$$\psi = A(t)\sin(ax)\sin(\pi z), \tag{31}$$

$$T = B_1(t)\cos(ax)\sin(\pi z) + B_2(t)\sin(2\pi z), \tag{32}$$

$$S = E_1(t)\cos(ax)\sin(\pi z) + E_2(t)\sin(2\pi z). \tag{33}$$

where the amplitudes A(t), $B_1(t)$, $B_2(t)$, $E_1(t)$ and $E_2(t)$ are functions of time and are to be deter-mined. Substituting above equations (31-33) in Eqs. (16-18), we get the following set of nonlinear autonomous differential equations

$$\frac{dA(t)}{dt} = F(t) \tag{34}$$

$$\begin{aligned} \frac{dF(t)}{dt} = &-\left(\frac{1}{\lambda_1} + \frac{\delta_1^2\lambda_2\,\mathrm{Pr}_D}{\delta^2\lambda_1}\right)F(t) - \frac{\delta_1^2\,\mathrm{Pr}_D}{\delta^2\lambda_1}A(t) \\ &- aRa_T\frac{\mathrm{Pr}_D}{\delta^2\lambda_1}\left(B_1(t) + \lambda_1\frac{dB_1(t)}{dt}\right) \\ &+ aRa_S\frac{\mathrm{Pr}_D}{\delta^2\lambda_1}\left(E_1(t) + \lambda_1\frac{dE_1(t)}{dt}\right), \end{aligned} \tag{35}$$

$$\frac{dB_1(t)}{dt} = -\left[\pi aA(t)B_2(t) + \left(\delta_2^2 - R_i\right)B_1(t) - 2aFA(t)\right], \tag{36}$$

$$\frac{dB_2(t)}{dt} = -\left[\left(4\pi^2 - R_i\right)B_2(t) - \frac{\pi a}{2}A(t)B_1(t)\right], \tag{37}$$

$$\frac{dE_1(t)}{dt} = -\left[aA(t) + \delta^2\tau E_1(t) + \pi aA(t)E_2(t)\right], \tag{38}$$

$$\frac{dE_2(t)}{dt} = -\left[4\pi^2\tau E_2(t) - \frac{\pi a}{2}A(t)E_1(t)\right]. \tag{39}$$

The above system of autonomous nonlinear differential equation is not suitable for analytical study. We use numerical method to solve the above set of nonlinear differential equation to find the amplitudes. After determining the amplitudes we can compute it to plot the graph for heat transfer, mass transfer, streamlines, isotherms, isohalines for un-steady case.

4.1 Heat and Mass Transports

The quantification of heat and mass transport is very important for the study of convection in porous media. This is because the onset of convection, as Rayleigh number is increased is more readily detected by its effect on the heat and mass transport. However in the basic state, heat and mass transfer is by conduction alone.

The Nusselt number and Sherwood number are de-fined by

$$Nu = 1 + \left[\frac{\int_0^{\frac{2\pi}{a}}\frac{\partial T}{\partial z}dx}{\int_0^{\frac{2\pi}{a}}\frac{dT_b}{dz}dx}\right]_{z=0}, \tag{40}$$

$$Sh = 1 + \left[\frac{\int_0^{\frac{2\pi}{a}}\frac{\partial S}{\partial z}dx}{\int_0^{\frac{2\pi}{a}}\frac{dS_b}{dz}dx}\right]_{z=0}, \tag{41}$$

Substituting the value of T , Tb, S and Sb in Eq. (40, 41), we get

$$Nu = 1 - \frac{2\pi B_2}{\sqrt{R_i}\cot\left(\sqrt{R_i}\right)}, \tag{42}$$

$$Sh = 1 - 2\pi E_2. \tag{43}$$

5. RESULTS AND DISCUSSION

In this section, we discuss the effect of parameters on the onset of convection, heat trans-port, mass transport. From linear stability analysis we plot neutral stability curve for the different values of parameters from the expression of thermal Rayleigh number. However from nonlinear analysis section, we solve the set of differential equations numerically and result is used to plot the curve for heat and mass transport with respect to time. We show the behaviour of heat and mass transport for the different values of parameter graphically more-over we made a comparison for the case with and without internal heat source for viscoelastic fluid. We also draw stream lines, isotherms and isohalines for unsteady case.

Figures (1-7) shows the neutral stability curve for different values of parameters. Figure (1) shows the effect of stress relaxation parameter on the onset of convection, we observe that the stress relaxation parameter advances the onset of convection for its increasing values. Figure (2) represents the effect of strain retardation parameter and from the graph it is clear that the strain retardation parameter delays the onset of convection for its increasing values. Figure (3) shows the effect of mechanical anisotropic parameter on the onset of convection and is observed from the graph that the mechanical anisotropic parameter advances the onset of convection for its increasing values it means that, if we fix the permeability in vertical direction and increase the permeability in horizontal direction or decrease the permeability in vertical direction and fix the permeability in horizontal direction the critical Rayleigh number decreases hence advances the onset of convection. Figure (4) shows the variation of thermal Rayleigh number for the different values of thermal anisotropic parameter and is clear from the graph that the thermal anisotropic parameter delays the onset of convection for its increasing values which means that if we fix the thermal diffusivity in vertical direction and increase the thermal diffusivity in horizontal direction or we decrease the thermal diffusivity in vertical direction and fix the thermal diffusivity in horizontal direction, the onset of convection delays. Figure (5) shows the variation of thermal Rayleigh number for the different value of internal heat source parameter and is found that internal heat source parameter advances the onset of convection for its increasing value that is if we increase the strength of the internal heat source the onset of convection advances starts early. Figure (6) shows the effect of Darcy-Prandtl number and is observe that Darcy-Prandtl advances the onset of convection for its increasing value this means that if we fix the Darcy number and increase the Prandtl number or we decrease the Darcy number and fix the Prandtl number the onset of convection advances. From Fig. (7) we observe that solute Rayleigh number delays the onset of convection for its increasing value. Figure (8) shows that the diffusivity ratio delays the onset of convection for its increasing value this indicates that, if we fix the solutal diffusivity and increase the thermal diffusivity in vertical direction or decrease the solutal diffusivity and fix the thermal diffusivity in vertical direction the onset of convection delays.

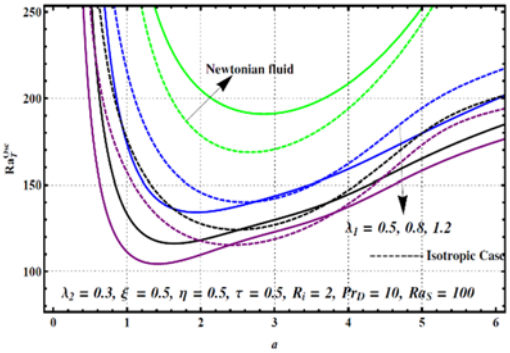

Fig. 1. Oscillatory neutral stability curves for different values of stress relaxation parameter λ_1.

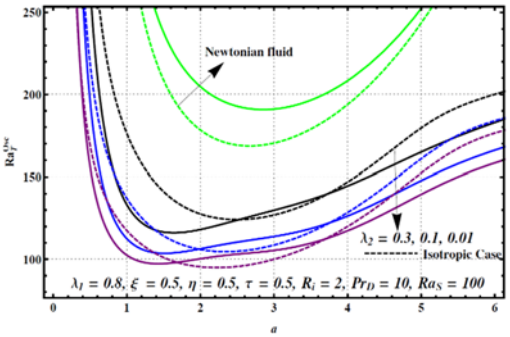

Fig. 2. Oscillatory neutral stability curves for different values of strain retardation parameter λ_2.

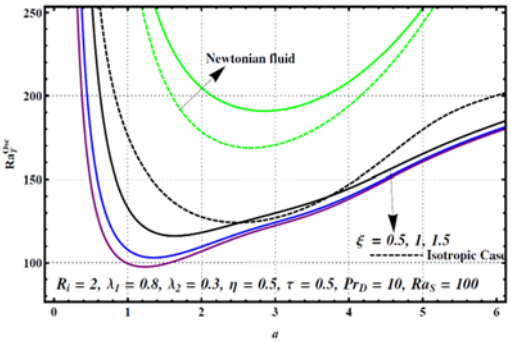

Fig. 3. Oscillatory neutral stability curves for different values of mechanical anisotropy parameter ξ.

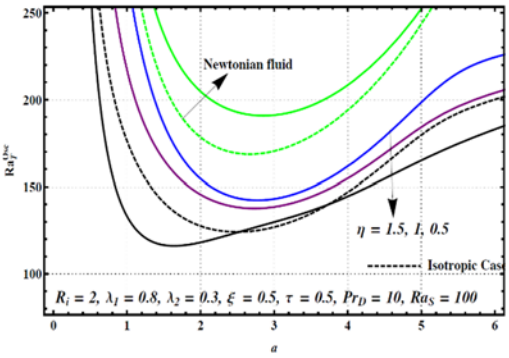

Fig. 4. Oscillatory neutral stability curves for different values of thermal anisotropy parameter η.

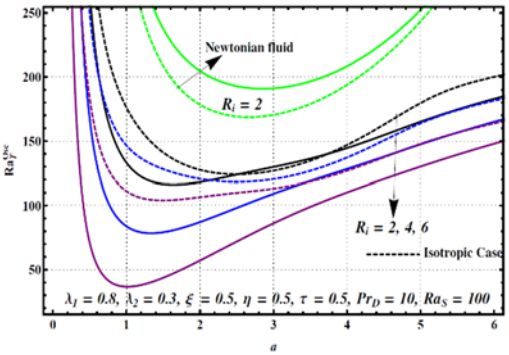

Fig. 5. Oscillatory neutral stability curves for different values of internal heat source parameter R_i.

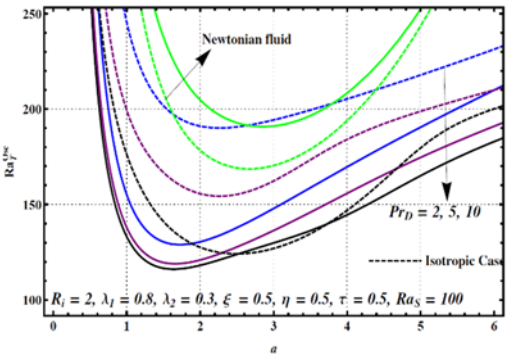

Fig. 6. Oscillatory neutral stability curves for different values of Darcy-Prandtl number Pr_D.

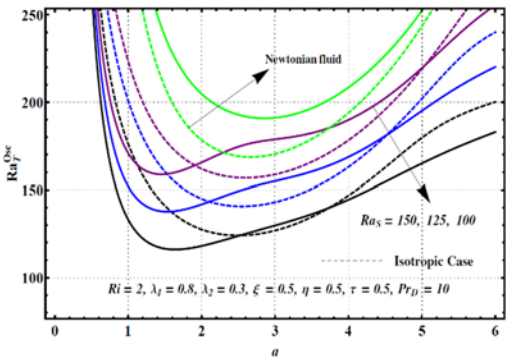

Fig. 7. Oscillatory neutral stability curves for different values of solute Rayleigh number Ra_S.

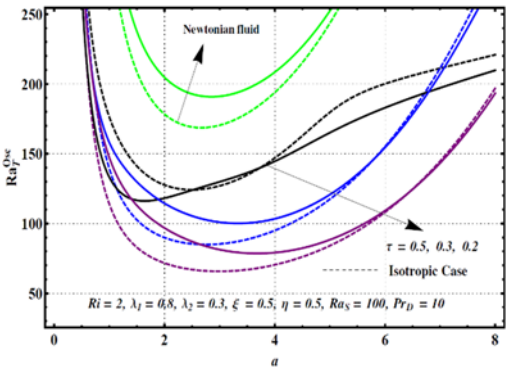

Fig. 8. Oscillatory neutral stability curves for different values of diffusivity ratio τ.

Variation of Nusselt number with respect to time for the different values of parameter is shown in the Figs. (9-16), initially Nusselt number oscillates with time and as time increases it became steady. Figure (9) shows the effect of stress relaxation parameter and is clear from the graph that the heat transport increases for the increasing value of stress relaxation parameter, moreover isotropic case is the extreme case, From Fig. (10) it is clear that the heat transport decreases for the increasing value of the strain retardation parameter, Fig. (11) shows the effect of mechanical anisotropic parameter on heat transport and is found that heat transport decreases for the increasing value of mechanical anisotropic parameter, that is, if we fix the permeability in the vertical direction and increase the permeability in horizontal direction heat transport de-creases or fix the permeability in horizontal direction and decrease the permeability in vertical direction heat transport decreases. Figure (12) shows the effect of thermal anisotropic parameter and is clear from the graph that the heat transport increases for the increasing value of thermal anisotropic parameter, that is, if we fix thermal diffusivity in vertical direction and increase the thermal diffusivity in horizontal direction heat transport increases or fix the thermal diffusivity in horizontal direction and decrease the thermal diffusivity in vertical direction heat transport increases. Figure (13) shows the effect of internal heat source and is found that the heat transport increases for the increasing value of internal heat source parameter that is if we increase the strength of internal heat source heat transfer increases. Figure (14) revealed that for the increasing value of Darcy-Prandtl number heat transport increases, this means if we increase the Prandtl number or decrease the Darcy number the heat transfer increases by keeping one of them fixed in the Darcy-Prandtl number. It should be mentioned here for the fixed value of varying parameter, heat transport is greater in isotropic case than anisotropic case, moreover when internal heat source is present, the heat transport is greater than the case when internal heat source is absent, from Fig. (15) we observe that for the increasing value of solute Rayleigh number the rate of heat transfer increases. From Fig. (16) we found that heat transfer decreases to increase in the diffusivity ratio it means that, if we fix thermal diffusivity in vertical direction and increase the solutal diffusivity the heat transfer decreases or fix

solutal diffusivity and increase the thermal diffusivity in vertical direction heat transfer increases.

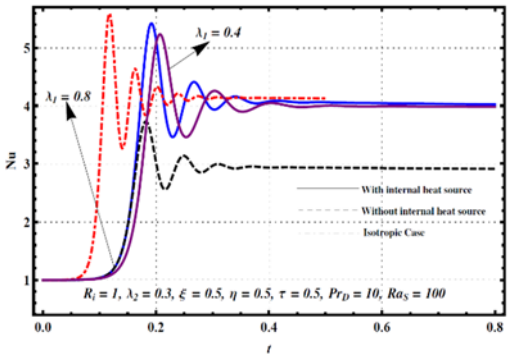

Fig. 9. Variation of Nusselt number with time for different values of λ_1.

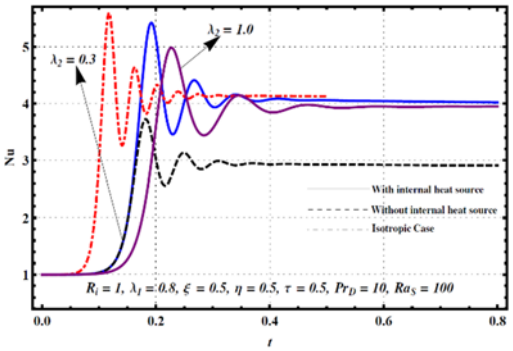

Fig. 10. Variation of Nusselt number with time for different values of λ_2.

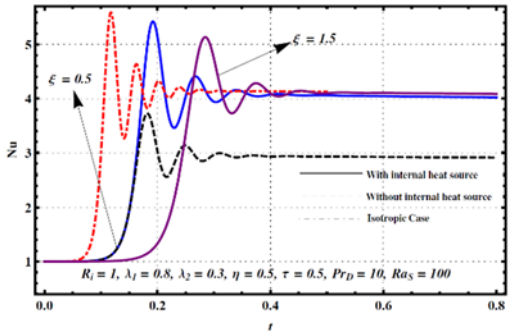

Fig. 11. Variation of Nusselt number with time for different values of ξ.

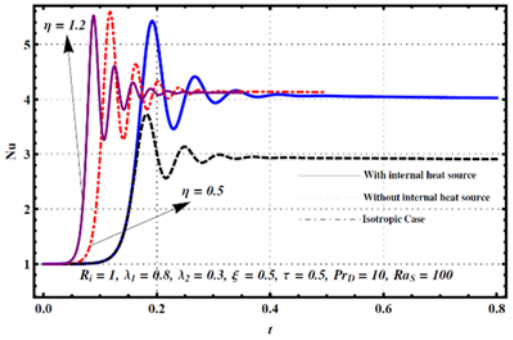

Fig. 12. Variation of Nusselt number with time for different values of η.

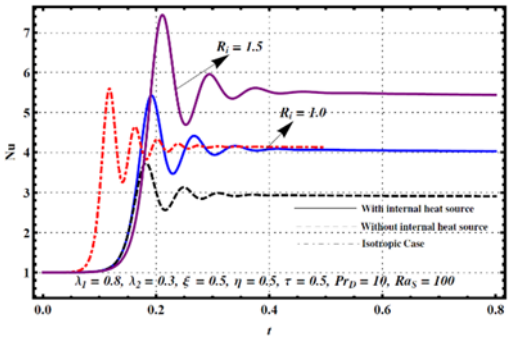

Fig. 13. Variation of Nusselt number with time for different values of R_i.

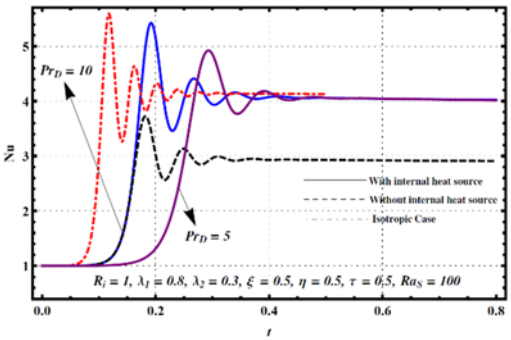

Fig. 14. Variation of Nusselt number with time for different values Pr_D.

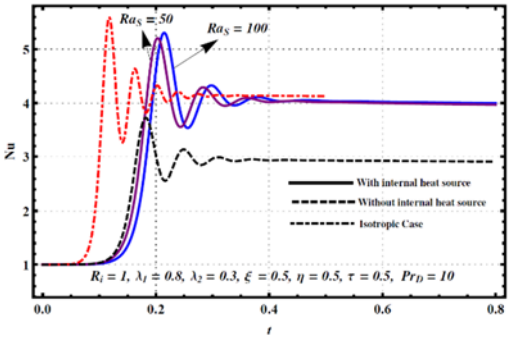

Fig. 15. Variation of Nusselt number with time for different values Ra_S.

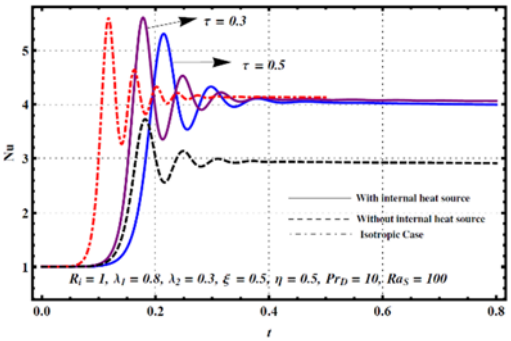

Fig. 16. Variation of Nusselt number with time for different values τ.

Variation of Sherwood number with respect to time for the different values of parameter is shown in the Fig. (17-24), initially Sherwood number

oscillates with time and as time increases it became steady. Figure (17) revealed the effect of stress re-laxation parameter and is observed from the graph that the mass transport increases for the increasing value of stress relaxation parameter, From Fig. (18) it is noted that the mass transport decreases for the increasing value of strain retardation parameter. Figure (19) shows the effect of mechanical anisotropic parameter on mass transport and is found that mass transport decreases for the increasing value of mechanical anisotropic parameter, if we fix the permeability in the vertical direction and increase the permeability in horizontal direction mass transport decreases or fix the permeability in horizontal direction and decrease the permeability in vertical direction mass transport decreases. Figure (20) shows the effect of thermal anisotropic parameter and is observed from the graph that the mass transport increases for the increasing value of thermal anisotropic parameter It means that if we fix thermal diffusivity in vertical direction and increase the thermal conductivity in horizontal direction mass transport increases or if we fix the thermal conductivity in horizontal direction and de-crease the thermal diffusivity in vertical direction mass transport increases. Figure (21) shows the effect of internal heat source and is found that the mass transport decreases for the increasing value of internal heat source parameter, it means that if we increase the strength of internal heat source mass transfer decreases. Figure (22) presents the effect of the Darcy-Prandtl number and is found that for the increasing value of Darcy-Prandtl number mass transport increases that is if we fix the Darcy number and increase the Prandtl number or decrease the Darcy number and fix the Prandtl number the mass transfer increases. It should be mentioned here for the fixed value of varying parameter mass transport is greater in isotropic case than anisotropic case, from Fig. (23) we found that for the increasing value of solute Rayleigh number the mass transfer increases. From Fig. (24) we see that mass transfer decreases for the increase in the diffusivity ratio, this indicates that if we fix thermal diffusivity and decreases the solutal diffusivity the mass transfer increases or we fix the solutal diffusivity and increases the thermal diffusivity mass transfer in-creases.

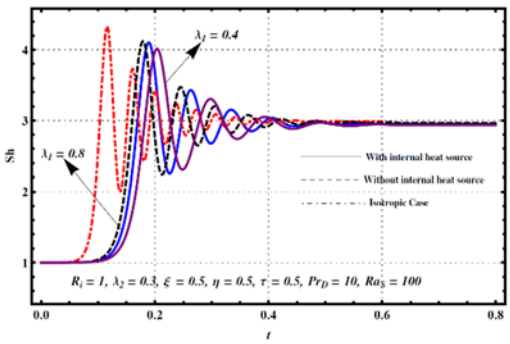

Fig. 17. Variation of Sherwood number with time for different values λ_1.

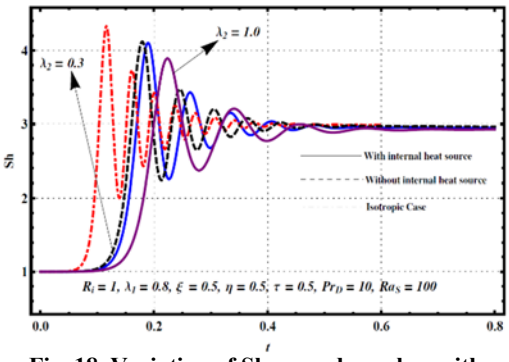

Fig. 18. Variation of Sherwood number with time for different values λ_2.

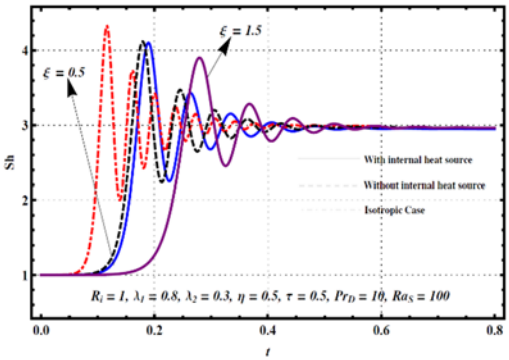

Fig. 19. Variation of Sherwood number with time for different values ξ.

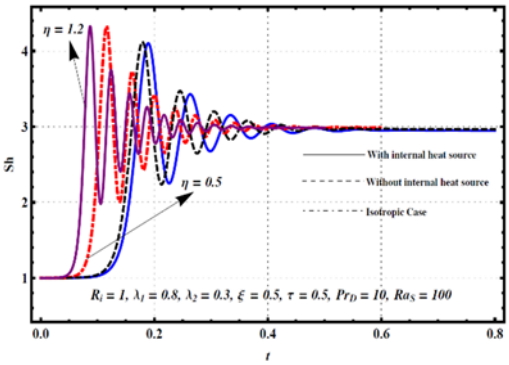

Fig. 20. Variation of Sherwood number with time for different values η.

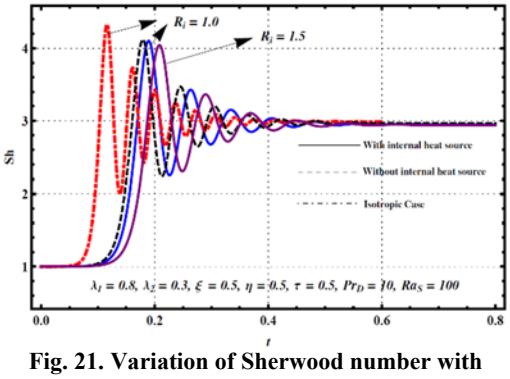

Fig. 21. Variation of Sherwood number with time for different values R_i.

Variation of stream lines, isotherms, isohalines at

different instant of time is shown graphically in Figs. (25–27) for the fixed value of parameters $R_i = 2$, $\lambda_1 = 0.8$, $\lambda_2 = 0.3$, $\xi = 0.5$, $\eta = 0.5$, $Ra_S = 100$, $\tau = 0.5$, $Pr_D = 10$. Fig. (25a-25c) revealed that the magnitudes of stream lines increases as time increases, Figs. (26a-26c) shows the variation of isotherms for the different instant of time and if clear that from the graph initially isotherms are flat and parallel shows the heat transport is only by conduction and as time increases isotherms starts oscillating and then forms contour showing that as time increases convection contributes in heat transport, similar behaviour is observed for isohalines in Figs. (27a-27c).

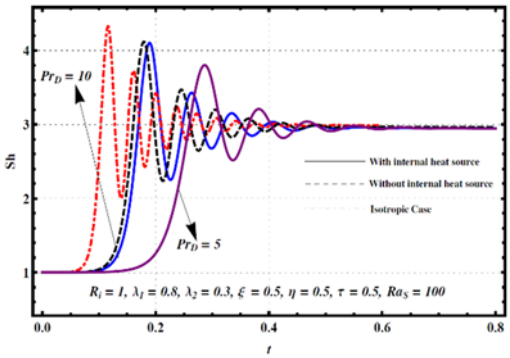

Fig. 22. Variation of Sherwood number with time for different values Pr_D.

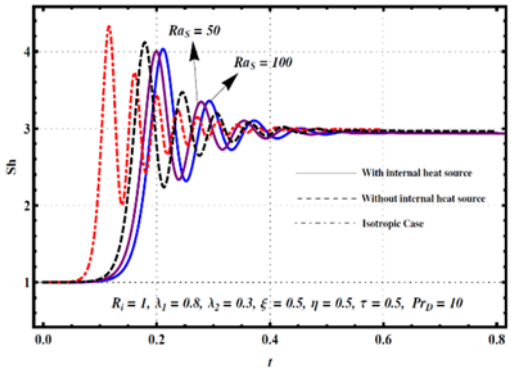

Fig. 23. Variation of Sherwood number with time for different values Ra_S.

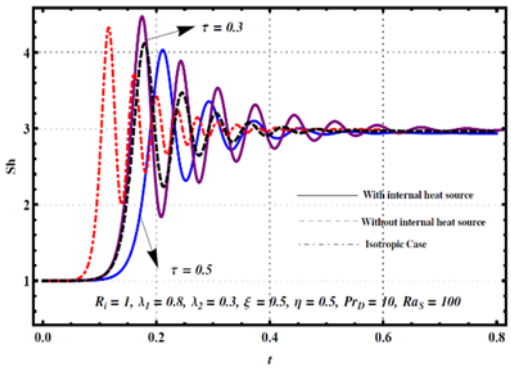

Fig. 24. Variation of Sherwood number with time for different values τ.

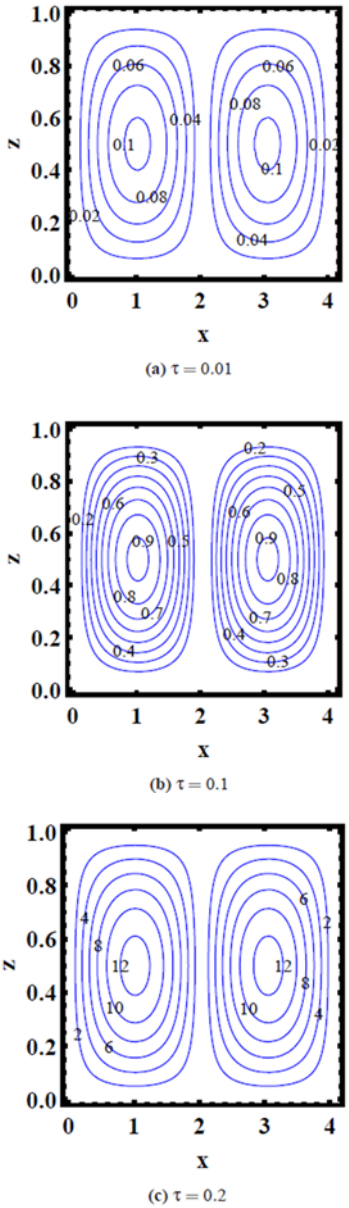

Fig. 25. Variation of stream lines with time.

6. CONCLUSIONS

We investigated the onset of convection for double diffusive convection with internal heat source in an infinite horizontal anisotropic porous layer which is heated and salted from below saturated with viscoelastic fluid. We also investigated the behaviour of heat and mass transfer and compare our result with isotropic case and Newtonian fluid. The following conclusions has been made from our analysis, for the increasing values of parameter

1. Relaxation parameter λ1: advances the onset of convection, heat transfer increases, mass transfer increases.
2. Retardation parameter λ2: delays the onset of convection, heat transfer decreases, mass transfer decreases.
3. Internal heat source parameter Ri: advances

the onset of convection, heat transfer increases, mass transfer decreases.

4. Mechanical anisotropic parameter ξ: advances onset of convection, heat transfer decreases, mass transfer decreases.
5. Thermal anisotropic parameter η: delays on-set of convection, heat transfer increases, mass transfer increases.
6. Darcy-Prandtl number PrD: advances onset of convection, heat transfer increases, mass transfer increases.
7. Diffusivity ratio number τ: delays onset of convection, heat transfer decreases, mass transfer decreases.
8. Solute Rayleigh number RaS: delays onset of convection, heat transfer increases, mass transfer increases.

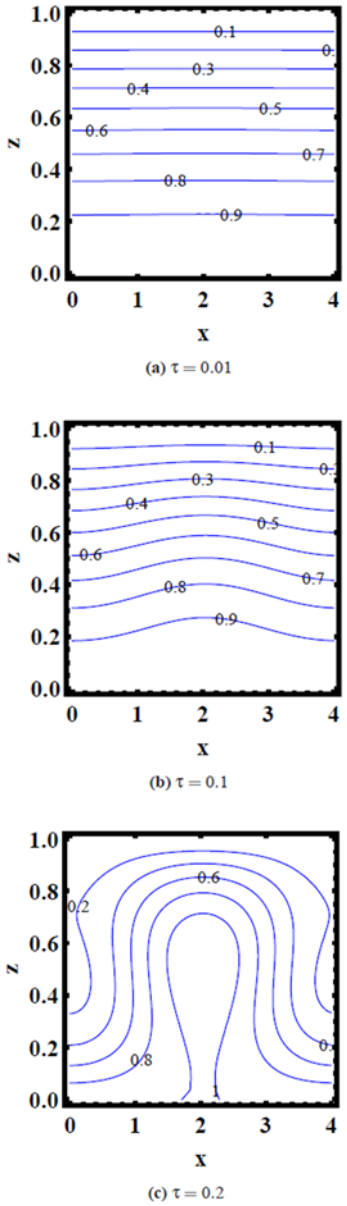

Fig. 26. Variation of isotherms with time.

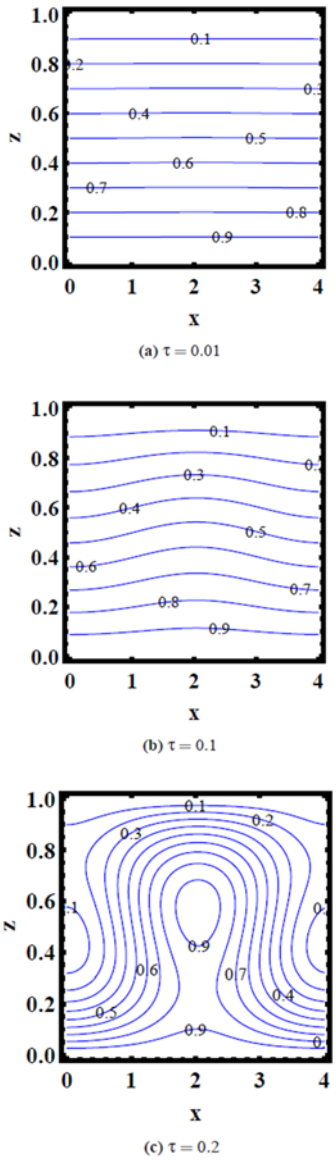

Fig. 27. Variation of isoconcentrations with time.

ACKNOWLEDGMENTS

Author Alok Srivastava gratefully acknowledges the financial assistance from Banaras Hindu University as a research fellowship during his Ph. D and from N.B.H.M. (D.A.E) during his Post Doctoral fellowship.

REFERENCES

Alex, S., P. Patil and K. Venakrishnan (2001). Variable gravity effects on thermal instability in a porous medium with internal heat source and inclined temperature gradient. *Fluid Dyn. Res. 29*, 1–6.

Altawallbeh, A., B. Bhadauria and I. Hashim (2014). Linear and nonlinear double-diffusive convection in a saturated anisotropic porous layer with soret effect and internal heat source. *International Journal of Heat and Mass*

Transfer 59, 103–111.

Bejan, A. (1978). Natural convection in an infinite porous medium with a concentrated heat source. *Journal of Fluid Mechanics 89*, 97–107.

Bhadauria, B. (2012). Double diffusive convec-tion in a saturated anisotropic porous layer with internal heat source. *Trans. Porous Media 92*, 299–320.

Bhadauria, B. (2016). Chaotic convection in a viscoelastic fluid saturated porous medium with a heat source. *Journal of Applied Mathematics Volume 2016*, Article ID 1487616.

Bhadauria, B., A. Kumar, J. Kumar, N. Sacheti and C. Pallath (2011). Natural convection in a rotating anisotropic porous layer with internal heat generation. *Transp. Porous Media 90*, 687–705.

Bhadauria, B., I. Hashim and P. Siddheshwar (2013). Study of heat transport in a porous medium under g-jitter and internal heating effects. *Transp Porous Med 96*(1), 21–37.

Capone, F., M. Gentile, and A. Hill (2011). Doublediffusive penetrative convection simulated via internal heating in an anisotropic porous layer with throughflow in an anisotropic porous layer with throughflow. *International Journal of Heat and Mass Transfer 54*, 1622–1626.

Cookey, C. I., V. B. O. Pepple, B. Obi and L. C. Eze (2010). Onset of thermal instability in a low prandtl number fluid with internal heat source in a porous medium. *American Journal of Scientific and In-Dustrial Research 1*, 18–24.

Gaikwad, S. and S. Kouser (2013). Onset of darcybrinkmanconvection in a binary viscoelastic fluid-saturated porous layer with internal heat source. *Heat Transfer-Asian Research 42*(8).

Gaikwad, S. and S. Kouser (2014). Double diffusive convection in a couple stress fluid saturated porous layer with internal heat source. *International Journal of Heat and Mass Transfer 78*, 1254–1264.

Griffiths, R. (1981). Layered double-diffusive convection in porous media. *J. Fluid Mech 102*, 221–248.

Hill, A. (2005). Double-diffusive convection in a porous medium with a concentration based internal heat source. *Proc. R. Soc. A 461*, 561–574.

Ingham, D. and I. Pop (2005). *Transport Phenomena in Porous Media*. Vol. III. Oxford: Elsevier.

Kang, J., C. Fu and W. Tan (2011). Thermal convective instability of viscoelastic fluids in a rotating porous layer heated from below. *J. Non-Newtonian Fluid Mech. 166*, 93–101.

Malashetty, M. and S. Kulkarni (2009). The convective instability of maxwell fluid-saturated porous layer using a thermal non-equilibrium model. *J. Non-Newtonian Fluid Mech. 162*, 29–37.

Malashetty, M. S., W. Tan and M. Swamy (2009). The onset of double diffusive convection in a binary viscoelastic fluid saturated anisotropic porous layer. Phys. *Fluids 21*, 084101.

Mulone, G. and B. Straughan (2006). An operative method to obtain necessary and sufficient stability conditions for double diffusive convection in porous media. *ZAMM 86*, 507–520.

Murray, B. and C. F. Chen (1989). Double- diffusive convection in a porousmedium. *J . Fluid Mech 201*, 147–166.

Narayana, M., P. Sibanda, S. Motsa and P. A. Lakshmi-Narayana (2012). Linear and non-linear stability analysis of binarymaxwell fluid convection in a porous medium. *Heat Mass Transfer 48*, 863–874.

Narayana, M., S. Gaikwad, P. Sibanda and R. Malge (2013). Double diffusive magneto-convection in viscoelastic fluids. *International Journal of Heat and Mass Transfer 67*, 194–201.

Nield, D. (1968). Onset of thermohaline con- vection in a porous medium. *Water Resour. Res 4*, 553–560.

Nield, D. and A. Bejan (2013). *Convection in Porous Media*, 4th edn. New York: Springer-Verlag.

Nouri-Borujerdi, A., A. Noghrehabadi and D. Rees (2007). Onset of convection in a horizontal porous channel with uniform heat generation using a thermal nonequilibrium model. *Transp Porous Med. 69*, 343–357.

Nouri-Borujerdi, A., A. Noghrehabadi and D. Rees (2008). Influence of darcy number on the onset of convection in porous layer with a uniform heat source. International *Journal of Thermal Sciences 47*, 1020–1025.

Parthiban, C. and P. Patil (1995). Effect of nonuniform boundary temperatures on thermal instability in a porousmedium with internal heat source. *Int. Comm. Heat Mass Transfer 22*, 683–692.

Poulikakos, D. (1986). Double diffusive convection in a horizontally sparsely packed porous layer. Int. Commun. *Heat Mass Transf. 13*, 587–598.

Rudraiah, N., P. Kaloni and P. Radhadevi (1989). Oscillatory convection in a viscoelastic fluid through a porous layer heated from below. Rheol. *Acta 28*, 48.

Rudraiah, N., P. Srimani and R. Friedrich (1982). Finite amplitude convection in a two-component fluid saturated porous layer. *Int. J. Heat Mass Transfer 25*(5), 715.

Saravanan, S. (2009). Thermal non-equilibrium porous convection with heat generation and density maximum. *Transp Porous Med 76*,

35–43.

Sekhar, G. and G. Jayalatha (2010). Elas- tic effects on rayleighbenard convection in liquids with temperature-dependent viscosity. *International Journal of Thermal Sciences 49*, 67–75.

Shivakumara, I. and S. Sureshkumar (2007). Convective instabilities in a viscoelastic-fluid-saturated porous medium with through-flow. *J. Geophys. Eng. 4*, 104–115.

Srivastava, A., B. S. Bhadauria and I. Hashim (2014). Effect of internal heating on double diffusive convection in a couple stress fluid saturated anisotropic porous medium. *Advances in Materials Science and Applications 3*(1), 24–45.

Tveitereid, M. (1977). Thermal convection in a horizontal porous layer with internal heat sources. *Int. J. Heat Mass Transfer 20*, 1045–1050.

Vadász, P. (2008). *Emerging Topics in Heat and Mass Transfer in Porous Media*. New York: Springer.

Vafai, K. (2005). *Handbook of Porous Media*. Boca Raton: Taylor and Francis (CRC).

Wang, W. and W. Tan (2008). Stability analysis of double-diffusive convection of maxwell fluid in a porous medium heated from below. *Phys. Lett. A 372*(17), 3046–3050.

Zhang, Z., C. Fu and W. Tan (2008). Linear and nonlinear stability analyses of thermal convection for oldroyd-b fluids in porous media heated from below. *Phys. Fluids 20*, 084103.